frontiers in Earth Science

ORIGINAL RESEARCH
published: 06 August 2021
doi: 10.3389/feart.2021.679862

Warning Decision-Making for Landslide Dam Breaching Flood Using Influence Diagrams

Yan Zhu[1,2,3], *Ming Peng*[1,2]*, *Peng Zhang*[4]* *and Limin Zhang*[5]

[1]Key Laboratory of Geotechnical and Underground Engineering of Ministry of Education, Tongji University, Shanghai, China, [2]Department of Geotechnical Engineering, College of Civil Engineering, Tongji University, Shanghai, China, [3]Shanghai Research Center of Ocean and Shipbuilding Engineering, China Shipbuilding NDRI Engineering Co., Ltd., Shanghai, China, [4]College of Civil Engineering, Qingdao University of Technology, Qingdao, China, [5]Department of Civil and Environmental Engineering, The Hong Kong University of Science and Technology, HKSAR, Hong Kong, China

Warning and evacuation are among the most effective ways for saving human lives and properties from landslide dam hazards. A new warning decision model for landslide dam break is developed using Influence Diagrams to minimize the total losses. An Influence Diagram is a simple visual representation of a decision problem. It analyzes the qualitative (causal) relationships between the variables *via* a logic diagram and determines the quantitative relationships *via* conditional probability and Bayes' theorem. The model is applied for the warning decision-making of the 2008 Tangjiashan landslide dam. The new model unifies the dam failure probability, evacuation, life loss, and flood damage in an Influence Diagram. Besides, a warning criterion is proposed for efficient decision-making. The model is more advanced than the decision tree since the inter-relationships of influence factors are qualitatively analyzed with causality connections and quantitatively analyzed with conditional probabilities. It is more efficient than a dynamic decision-making model (DYDEM) as it can directly calculate the three types of flood loss (i.e., evacuation cost, flood damage, and monetized life loss) and the expected total loss. Moreover, the probabilities of the influence factors leading to known results can be obtained through inversion analysis based on Bayesian theory. The new warning decision model offers an efficient way to save lives from landslide dam breaking and avoid unnecessary expenses from premature warning and evacuation.

Keywords: decision-making, Influence Diagrams, landslide dam, risk assessment, evacuation warning

OPEN ACCESS

Edited by:
Jie Dou,
China University of Geosciences, China

Reviewed by:
Faming Huang,
Nanchang University, China
Chong Xu,
National Institute of Natural Hazards, China

***Correspondence:**
Ming Peng
pengming@tongji.edu.cn
Peng Zhang
zhangpchn@qut.edu.cn

Specialty section:
This article was submitted to Geohazards and Georisks, a section of the journal Frontiers in Earth Science

Received: *12 March 2021*
Accepted: *07 July 2021*
Published: *06 August 2021*

Citation:
Zhu Y, Peng M, Zhang P and Zhang L (2021) Warning Decision-Making for Landslide Dam Breaching Flood Using Influence Diagrams. Front. Earth Sci. 9:679862. doi: 10.3389/feart.2021.679862

INTRODUCTION

A landslide dam is a naturally formed dam by rapid deposition of a landslide, avalanche, or debris flow, which blocks a river to form a natural lake. Unlike man-made earth and rockfill dam with well-designed drainage culverts and discharge spillway, a landslide dam often breaks soon after its formation, leading to a possibly abrupt and catastrophic breaching flood for downstream areas, just like the huge landslide dam triggered by the 1786 Ms 7.8 Luding-Kangding Earthquake. It breached soon after its formation and killed more than 100,000 people downstream (Zhang et al., 2016). In 1934, the Deixi Ms 7.5 earthquake triggered three landslide dams along the Minjiang River. The breaching flood of these three dams impacted the area as far as 800 km and drowned more than 3,000 people downstream (Liu et al., 2010; Peng and Zhang, 2012a).

Most landslide dams are short-lived. According to the statistical analysis of Shen et al. (2020) with 352 recorded cases, 30 and 48% of the landslide dams last only 1 day and 1 week, respectively. An extreme case is the Xiaolin Village landslide dam which was formed by the 2009 extreme Morakot Typhoon. It breached within 1 h after its formation and killed 384 people in the adjacent downstream Xiaolin Village (Li et al., 2011). To cope with these landslide dams, a timely warning is indispensable.

Nevertheless, the decision of dam break warning and evacuation should be very cautious and timely since it can be costly (Frieser, 2004; Peng and Zhang, 2013a, b; Shi et al., 2017). For instance, the breaking of the Tangjiashan landslide dam, triggered by the 2008 Ms 7.9 Wenchuan earthquake, forced as many as 300,000 people in Mianyang City (85 km downstream) to leave their homes for two weeks. The total evacuation expenses (including GDP interruption and evacuated expense) were estimated to be as much as RMB 1.2 billion. However, Mianyang City was not flooded, as the peak discharge of 7,800 m^3/ s was lower than that of the designed flood of 12,000 m^3/ s. Thus, a scientific decision on evacuation warning towards landslide dam break is crucial to achieving the minimal risk.

The existing studies on warning decision-making on dam breaking are divided into two categories: deterministic methods and probabilistic methods (Peng and Zhang, 2013a; Grant and Nover, 2019; Correa et al., 2020). Deterministic decision methods take water level and peak inflow rate and some other parameters as the indices for evacuation warning (Nielsen et al., 1994; Frieser, 2004; Zhai et al., 2018; Fan et al., 2019; Mandal et al., 2020). In some guidelines for dam safety, some subjective suggestions are offered for issuing dam break warning (Urbina and Wolshon, 2003; FEMA, 2004). Generally, the methods are quite intuitive and easy to apply. However, they fail to state the number of people to be evacuated and the best time to issue the warning. Furthermore, the uncertainties involved in dam break flood and human response are not evaluated.

In probabilistic decision methods, risk acceptance criteria based on fatality number and annual occurrence frequency were suggested for decision-making (BC Hydro, 1993; USBR, 1997; ANCOLD, 1998). Based on these criteria, the dam breaching risks higher than an acceptance level should be mitigated with structural or non-structural measures, including evacuation warnings. Su et al. (2011) have developed an early warning system of dam health with system engineering (e.g., integration control module, intelligent inference engine, and support base cluster) and artificial intelligent methods. Acosta-Coll et al. (2018) have reviewed the real-time early warning system design for pluvial flash floods and proposed a basic structure for an effective early warning system for pluvial flash floods. Fan et al. (2018) have studied the early warning of a dam break in a mountain river based on risk assessment *via* fuzzy analytic hierarchy process. Su et al. (2018) have developed an early warning model of deformation safety for roller compacted concrete arch dam by considering time-varying displacement data. Liu et al. (2018) have summarized the main early warning studies on flash flood with a systematic review on the early warning studies in China. Li et al. (2019) have conducted real-time warning and risk assessment of tailing dams based on dynamic hierarchy-grey relation analysis. Wang et al. (2020) have presented a method for early warning of crest cracking for high earth-rockfill dams *via* Bayesian parameter updating. The above existing studies on warning decision-making answered how likely the dam breaks or flash floods would occur but did not answer how much loss would be incurred. Thus, the optimal decision strategy to minimize the total loss cannot be quantitatively achieved, not to mention that the dynamic decision-making involved time-related losses.

Decision trees are often used for quantitative decision analysis because they are logical and intuitive (Frieser, 2004; Smith et al., 2006; Woo, 2008). Frieser (2004) has presented a decision tree on levee failure evacuation warning by considering three types of consequences: evacuation costs, flood damage, and loss of life. Time-dependent evacuation decisions can be analyzed using a multi-phase decision tree (Frieser, 2004). The alternatives in decision trees are assumed as independent, and the inter-relationships of influence factors are neglected. Peng and Zhang (2013a) and Peng and Zhang (2013b) have presented a decision-making model (DYDEM) based on dynamic risk assessment. The optimum time for evacuating the population at risk (PAR) is obtained by minimizing the expected total loss, which integrates the time-related probabilities and flood consequences. Based on DYDEM, Shi et al. (2017) have employed the pre-acquired terrain information to establish an efficient warning decision-making method. The method was applied to emergent evacuation warnings of the 2014 Hongshiyan landslide dam triggered by the Ms. 6.5 Ludian earthquake. DYDEM calculated the dam failure probability, human risk, economic loss, and evacuation cost with different methods. The expected total losses need to be calculated as the sum of the three types of expected losses (the product of the dam failure probability and the loss). This method is suitable for detailed case studies with sufficient investigated and simulated parameters. However, it may not be sufficient for efficient decision-making for short-lived landslide dam cases.

In this article, a new decision-making model is proposed based on Influence Diagrams. Influence Diagram integrates dam failure probability, the population at risk, fatality rate, and the three types of flood losses within one method. The new method would be much more precise than the decision tree and efficient than DYDEM. Firstly, the method of Influence Diagram is introduced and illustrated with an example. Secondly, a warning decision model is built by modifying the Bayesian network of a human risk assessment model (HURAM). Third, the model is applied to warning decision-making for the 2008 Tangjiashan landslide dam. Finally, the present model is compared with DYDEM and the decision tree method to illustrate the advantages. The new model provides an efficient and reliable method for warning decision-making for short-lived landslide dams. Both the time-related dam failure probability and three types of losses are involved within the new model.

METHODOLOGY

Influence Diagram

Background of the Influence Diagram

Influence Diagram, first presented by Howard and Matheson (2005), is a method to solve complex decision problems by

considering the inter-relationships of influence factors and their uncertainties. An Influence Diagram is a simple visual representation of a decision problem. It offers an intuitive way to identify and display the essential elements, including decisions, uncertainties, objectives, and how they influence each other. It adopts the form of a logic diagram to analyze the qualitative (causal) relationship between the variables. It uses conditional probability and Bayes' theorem to analyze the quantitative relationship between the variables.

The influence graph is an extension of the Bayesian network method by employing decision nodes and utility function nodes. The application procedure of the Influence Diagram is divided into three steps: establishing the Influence Diagram structure by causal analysis of variables; obtaining the prior probability values based on multi-source information such as statistic data, theoretic analysis, and numerical simulation; obtaining the posterior probabilities with evidence according to Bayes' theorem.

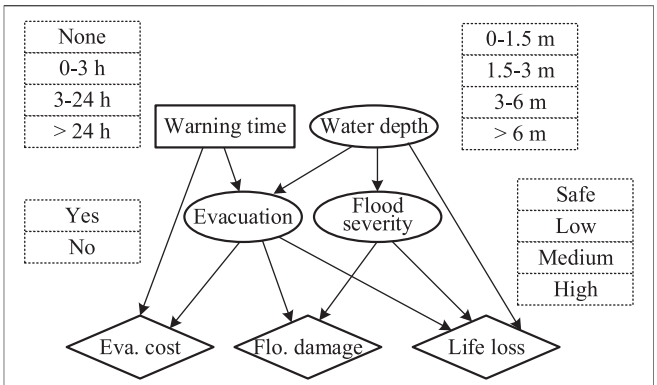

FIGURE 1 | An example of Influence Diagram: eva. = evacuation and flo. = flood.

Theoretical Introduction

Assume that an Influence Diagram has l decision nodes of D_1, D_2,. . .D_l, m chance nodes of C_1, C_2,. . .,C_m, and n utility function nodes U_1, U_2,. . .,U_n. The value of each utility function node given any combination of decision nodes and chance nodes is calculated as follows

$$U_k|_{\mathbf{D},\mathbf{X}_q} = U_k[\boldsymbol{\pi}(U_k)]P\left[\boldsymbol{\pi}(U_k)|\mathbf{D},\mathbf{C}_q\right], \tag{1}$$

where U_k is the *kth* utility function node, $\boldsymbol{\pi}(U_k)$ is the parent node set of U_k, $\mathbf{D}$ is the decision node set (D_1, D_2,. . .D_l), $\mathbf{C}_q$ is the set of chance nodes with evidences, and U_k $[\boldsymbol{\pi}(U_k)]$ is the utility function of $\boldsymbol{\pi}(U_k)$.

$$\begin{aligned} P\left[\boldsymbol{\pi}(U_k)\middle|\mathbf{D},\mathbf{C}_q\right] &= \frac{P\left[\boldsymbol{\pi}(U_k),\mathbf{D},\mathbf{C}_q,\mathbf{C}_r\right]}{P\left(\mathbf{D},\mathbf{C}_q\right)} \\ &= \frac{P\left[\boldsymbol{\pi}(U_k),\mathbf{D},\mathbf{C}_q,\mathbf{C}_r\right]}{\sum_{\boldsymbol{\pi}(U_k),\mathbf{C}_r} P\left[\boldsymbol{\pi}(U_k),\mathbf{D},\mathbf{C}_q,\mathbf{C}_r\right]}, \end{aligned} \tag{2}$$

where $\mathbf{C}_r$ is the set of chance nodes without evidences (stochastic valuables) and P $[\boldsymbol{\pi}(U_k), \mathbf{D}, \mathbf{C}_q, \mathbf{C}_r]$ is the joint probability of all parameters (nodes) in an Influence Diagram.

Express all types of nodes as a set $\mathbf{X}$ (X_1, X_2, . . ., X_N), in which $N = l + m + n$. The joint probability P (X_1, X_2, . . ., X_N) can be expressed as the products of the conditional probability of each node given its parents (Jensen, 2001):

$$P(X_1, X_2, \ldots, X_N) = \prod_{i=1}^{n} P(X_i|\pi(X_i)), \tag{3}$$

where $\pi(X_i)$ is the set of all the parents of X_i. For discrete state Bayesian network, the basic parameters of a Bayesian network are expressed as follows (Zhang and Guo, 2006):

$$\theta_{ijk} = P\left(X_i = k\middle|\pi(X_i) = j\right), \tag{4}$$

where k and j are the state numbers of the node X_i and its parents, respectively. According to the Bayesian theorem, the posterior probability of the parameter vector is given by the following (Zhang and Guo, 2006):

$$P(\boldsymbol{\theta}|D) \propto P(\boldsymbol{\theta}) \prod_{i=1}^{n} \prod_{j=1}^{q_i} \prod_{k=1}^{r_i} \theta_{ijk}^{m_{ijk}}, \tag{5}$$

in which $\boldsymbol{\theta}$ is the vector of θ_{ijk}, P($\boldsymbol{\theta}$) is the prior probability of $\boldsymbol{\theta}$, and m_{ijk} is the number of samples with $X_i = k$ and $\pi(X_i) = j$.

TABLE 1 | The prior conditional probability table of evacuation using HURAM (Peng and Zhang, 2012b).

D_w (m)		0–1.5 (0.378)*				1.5–3 (0.406)*			
W_t (h)		0	0–3	3–24	>24	0	0–3	3–24	>24
Evacuation	Yes	0.134	0.513	0.979	1.000	0.091	0.473	0.979	1.000
	No	0.866	0.487	0.021	0.000	0.909	0.527	0.021	0.000
D_w (m)		3–6 (0.187)*				>6 (0.029)*			
W_t (h)	0	0–3	3–24	>24	0	0–3	3–24	>24	
Evacuation	Yes	0.028	0.407	0.975	1.000	0.012	0.371	0.973	1.000
	No	0.972	0.593	0.025	0.000	0.988	0.629	0.027	0.000

Note: the prior probability values in the brackets are obtained based on statistical data.

An Illustrated Example of Influence Diagram

The Example

Figure 1 shows a simple example of using an Influence Diagram to make warning decisions. Four influence factors are considered, among which W_t is the decision node (with 4 states) and the water depth (D_w) (with 4 states), evacuation (with 2 states), and flood severity (with 4 states) are the chance nodes. The utility function notes are three types of losses: evacuation cost, flood damage, and monetized life loss. The optimal decision is achieved to minimize the total expected loss, which is the sum of the three types of losses. This target is realized with three steps: building the Influence Diagram, quantifying the Influence Diagram with prior probabilities, and calculating the total expected loss with different warning times by Bayesian updating.

The Structure of Influence Diagram

The Influence Diagram structure is established by considering the causal relationships of the variables (**Figure 1**). In the Influence Diagram, W_t influences evacuation and evacuation cost. An earlier warning would evacuate more people and incur more evacuation costs. Sufficient evacuation reduces flood damage and life loss but increases the evacuation cost at the same time. A larger water depth incurs less efficiency of evacuation, larger flood severity, and more life loss. Flood severity, determined by the building inundation and damage (Peng and Zhang, 2013a; Peng and Zhang, 2013b), directly influences the flood damage and life loss.

The Prior Probability of the Influence Diagram

The prior (conditional) probabilities of the three chance nodes (D_w, evacuation, and flood severity) are obtained according to Peng and Zhang (2012b) and Peng and Zhang (2012c), as shown in **Tables 1**–**2**. The prior probabilities of D_w are obtained based on statistical data (**Table 1**). The prior condition probabilities of evacuation (**Table 1**) are regarded as the probabilities when the available time is larger than the demand time, which will be introduced later. The prior condition probabilities of the flood severity (**Table 2**) are obtained based on a matrix of building inundation and building damage, according to Peng and Zhang (2012b).

TABLE 2 | The prior conditional probability table of flood severity using HURAM (Peng and Zhang, 2012b).

D_w (m)		0–1.5	1.5–3	3–6	>6
Flood severity	Safe	0.608	0.353	0.168	0.081
	Low	0.284	0.171	0.099	0.081
	Medium	0.108	0.476	0.529	0.481
	High	0.000	0.000	0.204	0.357

The evacuation cost consists of GDP interruption loss and people resettlement costs. The flood damage is counted by the damage of movable properties in this study since the unmovable properties cannot be saved by warning and evacuation. Human life is monetized for evacuation decision-making. The value of human life is counted as the GDP per person (GDP_P) and the average longevity (L_{av}) (Frieser, 2004; Jonkman, 2007). For example, the GDP_P and L_{av} in Mianyang City, China, are RMB 13,745 and 75 years in 2008 (Mianyang Bureau of Statistics, 2008). Thus, the value of one person is estimated as RMB 1.03 million. Suppose that the population at risk (P_{ar}) is 1,000 in this case. The prior utility functions of evacuation cost, flood damage, and life loss are calculated based on Peng and Zhang (2013a), as shown in **Tables 3**–**4**, respectively.

The Total Expected Loss as a Function of Warning Time

Finally, the total expected loss (L_T) is calculated as follows:

$$L_T = C + P_f(D_M + M_L), \tag{6}$$

where C denotes the evacuation cost, D_M is the movable flood damage, M_L is the monetized life loss, and P_f is the probability of landslide dam failure. The three types of flood losses are posterior values calculated by updating the prior values based on Bayes' theorem. In this case, we can obtain each of the flood losses, according to **Eqs. 1**–**4**. Take the flood damage D_M as an example. According to **Figure 1**, D_M is calculated as follows:

$$D_M\big|_{(W_t,D_w)} = \sum_{W_t,E_{va}} D_M(E_{va},F_S)P(E_{va},F_S|W_t,D_w), \tag{7}$$

where E_{va} is the evacuation, F_s is the flood severity, and D_M (E_{va}, F_s) is the flood damage as a function of E_{va} and F_s, which can be found in **Table 3**. The conditional probability P (E_{va}, F_s |W_t, D_w) is calculated as follows:

$$P(E_{va},F_S|W_t,D_w) = \frac{P(E_{va},F_S,W_t,D_w)}{P(W_t,D_w)} = \frac{P(E_{va},F_S,W_t,D_w)}{\sum_{W_t,D_w} P(E_{va},F_S,W_t,D_w)}. \tag{8}$$

According to Equation (3), the joint probability P (E_{va}, F_s, W_t, D_w) is as follows:

$$P(E_{va},F_S,W_t,D_w) = P(W_t)P(D_w)P(E_{va}|W_t,D_w)P(F_S|D_w), \tag{9}$$

where P(W_t) = 1 for decision node; P (D_w) can be found in **Table 1**, and P (E_{va}|W_t, D_w) and P(F_s|D_w) in **Table 2**.

TABLE 3 | Prior probability of evacuation cost and flood damage with P_{ar} of 1,000 based on Peng and Zhang (2013a).

Evacuation	Yes				No			
Warning (h)	None	0–3	3–24	>24	None	0–3	3–24	>24
Evacuation (million RMB)	0	0.343	0.428	0.526	0	0.155	0.188	0.226
Flood severity	Safe	Low	Med	High	Safe	Low	Med	High
Flood damage (million RMB)	0.0	0.0	0.0	0.0	0.0	1.345	3.137	4.482

Note: the evacuation cost consists of GDP interruption loss and people arrangement fee for people who have evacuated only.

TABLE 4 | Prior probability of life loss with P_{ar} of 1,000 based on Peng and Zhang (2013a).

Evacuation	**No**							
Flood severity	**Low**				**Medium**			
D_w (m)	0–1.5	1.5–3	3–6	>6	0–1.5	1.5–3	3–6	>6
Fatality rate	0.19	1.59	5.74	12.52	0.19	7.42	38.88	73.20
Monetized life loss	196	1,638	5907	12896	196	7643	40046	75396

Note: the fatality rate of the evacuated people and the people in the safe flood severity is zero.
The fatality rate in the high flood severity zone is a constant value of 90.78% (Peng and Zhang, 2013a).

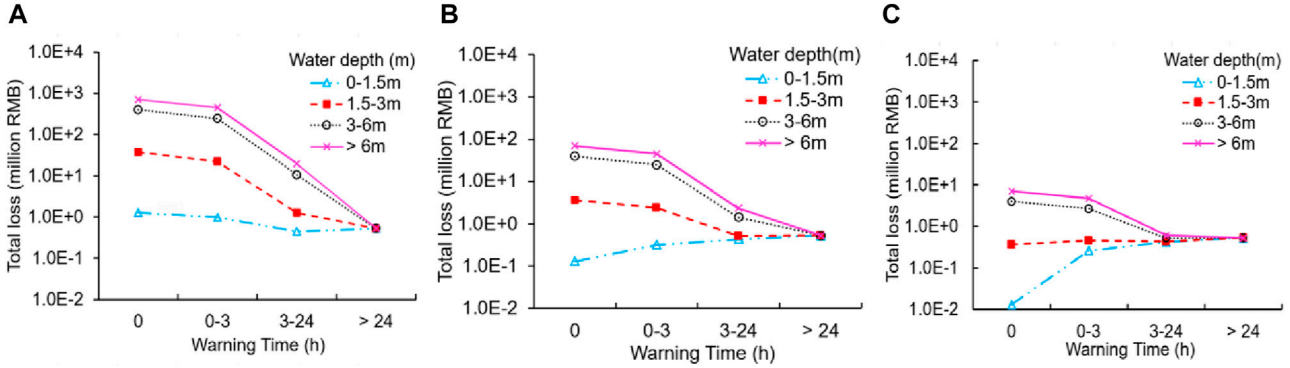

FIGURE 2 | Variation of total loss with W_t and D_w: **(A)** P_f = 1; **(B)** P_f = 0.1; **(C)** P_f = 0.01.

Figure 2 shows the total expected loss (L_T) with different values of W_t, D_w, and P_f. Generally, L_T increases with D_w and P_f. The influence of W_t on L_t is more complicated. When P_f and D_w are large, L_T decreases with W_t, as L_T is dominated by M_L and D_M. When P_f and D_w are small, L_T decreases with W_t. When P_f and D_w are relatively large, L_T decreases and then increases with W_t. For instance, minimal L_T is achieved as 0.53 million RMB when $W_t > 24$ h, in the case of $P_f = 1$ and $D_w = 3$–6 m; minimal L_T can be ignored with no warning when P_f reduces to 0.01 and D_w is 0–1.5 m.

THE NEW DECISION-MAKING MODEL

The target of the decision-making model is to find the optimal time for issuing a warning to minimize the risk (R) or the expected total loss (L_T):

$$R = L_T(t) = \int_{t_f=0}^{\infty} \left\{ C(W_t) + P_f\left(t_f\right)\left[D_M(W_t) + M_L(W_t)\right] \right\} dt_f \tag{10}$$

$$W_t = t - t_f, \tag{11}$$

where t is the moment for issuing warning. t_f is the moment of dam failure. W_t denotes the warning time. $P_f(t_f)$ denotes the failure probability of the landslide dam before t_f as a time series. $C(W_t)$, $D_M(W_t)$, and $M_L(W_t)$ are evacuation cost, movable flood damage, and monetized life loss as functions of W_t, respectively. Note that the unmovable damage is not involved since it cannot be mitigated by warning and evacuation. Normally, $C(W_t)$ increases but $D_M(W_t)$ and $M_L(W_t)$ decrease with W_t.

Decision Criterion

The decision criterion is to find the optimal time for issue warning to minimize $L_T(t)$ or $L_T(t_f + W_t)$. When $P_f(t_f)$ is very small (e.g., at the dam formation moment with shallow water level), $L_T(t)$ is dominated by $C(W_t)$ and the minimal $L_T(t)$ is achieved at $W_t = 0$, which means no warning is necessary. With the increase of $P_f(t_f)$, $L_T(t)$ increases. When $L_T(t)$ achieves the minimal value with $W_t > 0$ for the first time, which means early warning is necessary, we need to warn the people before this moment, t_{cr}. A warning is not needed before t_{cr} and needed after t_{cr}:

$$L_T(t_{cr}) < L_T(t_{cr} + W_t) \text{ and } L_T(t) > L_T(t + W_t), \text{for any } W_t > 0 \text{ and } t > t_{cr}. \tag{12}$$

Since $P_f(t)$ monotonously increases with t before dam failure, we can first find the critical failure probability P_{fcr} in the Influence Diagram (to be introduced later) and then obtain t_{cr} as the inverse function of $P_f(t)$.

$$t_{cr} = P_f^{-1}\left(P_{fcr}\right). \tag{13}$$

The Human Risk Analysis Model

In **Eq. 10**, $C(W_t)$, $D_M(W_t)$, and $M_L(W_t)$ can be calculated using a new warning decision model *via* Influence Diagram, which is built by improving the Bayesian network of a human risk

assessment model, HURAM (Peng and Zhang, 2012b; Peng and Zhang, 2012c). The logic structure of HURAM is shown in **Figure 3**. People in the flooded area are called population at risk (P_{ar}). A part of P_{ar} evacuates from the flooded areas to be safe if the available time is larger than the demand time. The other people, who stay in the flooded area, are defined as exposed people. The exposed people may take shelter inside buildings. If so, their safety depends on the building inundation and damage. There are four flood severity zones: safe, low, medium, and high. The fatality ratio of the four zones is quantified based on statistical data, as shown in **Figure 3** (Peng and Zhang, 2012b). HURAM model is able to estimate the human risk (i.e., probability of life loss) by considering fourteen parameters and their interrelationship. The model is validated in several cases (Peng and Zhang, 2012b; Peng and Zhang, 2013b; Shi et al., 2017).

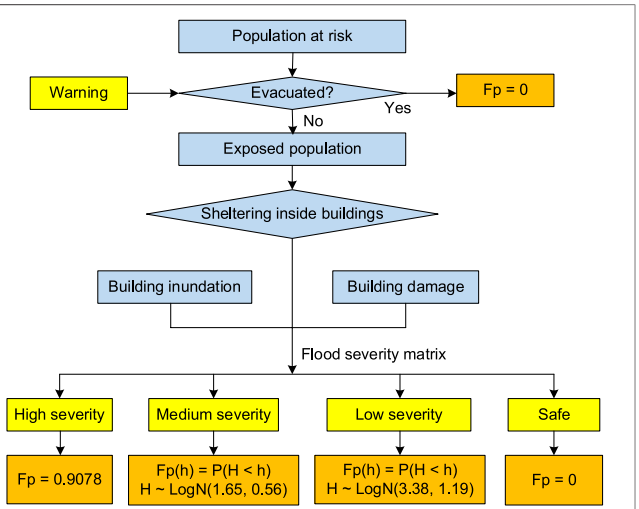

FIGURE 3 | The framework of the human risk assessment model for a landslide dam (modified from Peng and Zhang, 2012b; Peng and Zhang, 2013a).

New Decision-Making Model With Improvements on HURAM

A new decision-making model (DEMID) (**Figure 4**) is developed based on Influence Diagram. It improves the Bayesian network of HURAM mainly in five aspects: changing the states of the "warning time" node; removing the "time of a day" node; changing the functions of the "evacuation" node; adding two chance nodes "dam failure probability" and "population at risk"; adding three utility function nodes "evacuation cost," "flood damage," and "monetized life loss."

Changing the States of the "Warning Time" Node

"Warning time," an originally chance node, is changed to a decision node. Originally in HURAM, "warning time" has five states: 0–0.25 h, 0.25–1 h, 1–3 h, 3–6 h, and >6 h. It is an intermediate node with two parent nodes of "time of a day" and "distance to dam site," which meant that the available W_t is influenced by "time of a day" and the "distance to dam site" (Peng and Zhang, 2012a). In DEMID, W_t is set as a decision node in the Influence Diagram with seven states: 0–0.25 h, 0.25–1 h, 1–3 h, 3–6 h, 6–12 h, 12–24 h, and >24 h. Two more states with longer warning times are added as more time needs to be offered for people to save their properties.

Removing the "Time of a Day" Node

"Time of a day," an originally chance node, is removed. In HURAM, the node "time of a day" had three states: 8:00–17:00, 17:00–22:00, and 22:00–8:00. It was a parent node of three intermediate nodes: "warning time," "evacuation," and "sheltering inside buildings". In DEMID, the lead time for

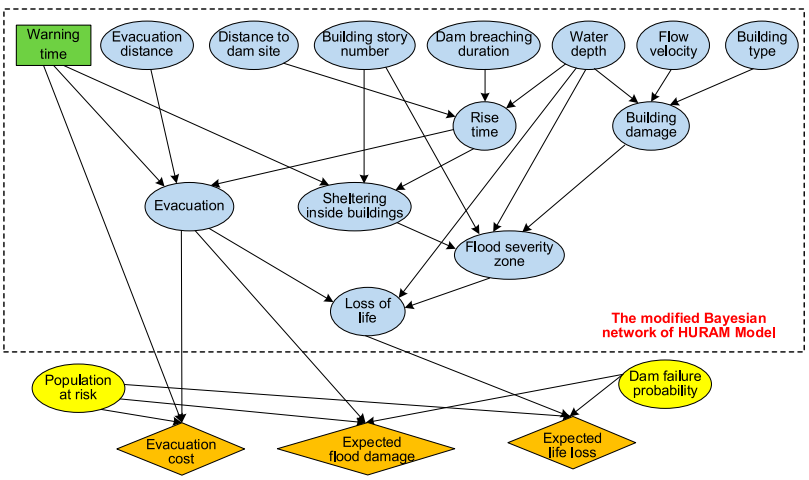

FIGURE 4 | The decision-making model based on Influence Diagram.

decision-making was often on the order of days, making the simulation of warning and evacuation rather complex. Besides, we can choose daytime for issuing a warning. Thus, the chance node of "time of a day" in the Influence Diagram was removed (Peng and Zhang, 2013a).

Changing the Function of "Evacuation" Node

The warning transmitting time distribution and response time distribution are changed. In HURAM, a successful evacuation is defined as the available time ($W_t + R_t$) larger than demand time ($T_t + S_t + E_t$) (Peng and Zhang, 2013a):

$$W_t + R_t > T_t + S_t + E_t, \tag{14}$$

where W_t is the warning time; R_t is the flood rise time (the time for the flood water level rising to a critical level causing threat to human life, 1.5 m is assumed); T_t is the warning transmitting time (the duration from issuing the warning to the receipt by the people at risk); S_t is the response time (the time for people to confirm the warning, prepare for evacuation and wait for family members); E_t is the evacuation time (the time for the people to mover to safe places).

In HURAM, the warning transmitting distribution was W (3.5, 0.6), W (2.0, 0.5), and W (1.3, 0.7) for times of a day of 08: 00–17:00, 17:00–22:00, and 22:00–08:00, respectively. Here W (a, b) denotes a Weibull distribution with coefficients a and b:

$$P(t) = 1 - \exp\left(-at^b\right). \tag{15}$$

In DEMID, we use W (1.3, 0.7) only for safety and to avoid complex calculations (Peng and Zhang, 2013b). W (1.3, 0.7) is suggested for moderately rapid warning by Lindell et al. (2007).

In HURAM, the response time distribution is assumed as W (4, 1) for emergent dam break situation, with a mean value and standard deviation of 0.25 and 0.25 h, respectively. In emergent cases, people have no more time to rescue properties. However, in DEMID, the government should consider offering more time for people to save properties and prepare daily belongings. A distribution of W (0.085, 2.55) is chosen according to the practices of hurricane evacuation (Lindell et al., 2007). In this case, the mean value and a standard deviation of 2.33 and 0.98 h are considered, respectively.

Adding Two Chance Nodes of "Population at Risk" and "Dam Failure Probability"

Two chance nodes, namely, the "population at risk" and "dam failure probability," are added to the Influence Diagram. In HURAM, the flooded areas are divided into subareas with different populations at risk (P_{ar}) and flood parameters. The human risk (R_H) is calculated as the sum of the expected life loss (L_i) in each subarea:

$$R_H = \sum_{i=1}^{n} L_i = \sum_{i=1}^{n} P_f P_{l|f} P_{ar}, \tag{16}$$

where $P_{l|f}$ is the conditional probability of life loss when the dam fails. Three steps are needed: firstly, dividing the flooded area into subareas with different P_{ar}s; secondly, obtaining $P_{l|f}$ *via* the Bayesian network in HURAM; finally, calculating R_H with P_f according to **Eq. 16**.

In DEMID, R_H is directly calculated as shown in **Figure 4** by adding two chance nodes: "population at risk" with five states (1, 1E2, 1E4, 1E6, and 1E8) and "dam failure probability" with seven states (0, 1E-5, 1E-4, 1E-3, 1E-2, 1E-1, and 1). The flood area need not to be divided into subareas as in HURAM. The distribution of P_{ar} and the flood parameters (D_w, flow velocity, and rise time) are taken as probabilities in the Influence Diagram. Despite discrete states in the two added nodes, all continuous values can be achieved by the weighted average of the two closest states by solving the following equation:

$$P = P_i S_i + P_{i+1} S_{i+1} \tag{17}$$

$$P_i + P_{i+1} = 1, \tag{18}$$

where P_i and P_j are two probability weights of the two closest states and S_i and S_j are the two state values. For instance, P_{ar} with 30,000 could be expressed as 0.9798*1E4 + 0.0202*1E6. Besides, the human risk could be assessed *via* DEMID; also, the expected flood damage and evacuation cost could be evaluated at the same time by employing three utility function nodes as follows.

Adding Three Utility Function Nodes

Three utility function nodes, namely, "evacuation cost," "expected flood damage," and "expected life loss," are added in the new model. The evacuation cost is the sum of the initial costs (C_i) and GDP interruption (C_{GDP}) (Peng and Zhang 2013a):

$$C = C_i + C_{GDP}. \tag{19}$$

C_i is the evacuation expenses, such as temporary resettlement fee (e.g., accommodation, food, and compensation) and public maintenance fee (e.g., security and medical care), and can be calculated as follows:

$$C_i = cP_{eva}(W_t + 3), \tag{20}$$

where c is the expense per person per day (e.g., RMB 60 or US$ 9.5 per person per day for the evacuation caused by the 2008 Tangjiashan landslide dam); P_{eva} is the number of evacuated people, which is estimated using the HURAM; W_t is the warning time in days. The 3-day period is taken as the minimum period of time between the predicted moment of flooding and the return of the residents (Frieser, 2004). The GDP interruption (C_{GDP}) is calculated as follows:

$$C_{GDP} = \frac{GDP_P}{365}(PAR)(W_t + 4), \tag{21}$$

where GDP_P is the GDP per capita and the interrupted time.

The moveable flood damage D_M is assumed to be proportional to the number of the people who neither evacuated nor sheltered in safe zones (in the building story beyond the inundation height) (Peng and Zhang, 2013a):

$$D = (1 - P_{eva})\left(1 - P_{safe}\right)(PAR)\alpha I_p, \tag{22}$$

where P_{safe} is the ratio of the people taking shelter in the safe zones; α is the proportion of properties that can be transferred

(0.1 is assumed); I_p is the property of each person, which is calculated approximately as the cumulative net income (i.e., income minus spending) per person (Peng and Zhang, 2013a):

$$I_p = (I - S)n, \tag{23}$$

where I and S are the average income and spending per person; n is the average working period per person (e.g., 20 years). For instance, in 2008, Mianyang City, Sichuan Province, China, I_p = 4,482 * 20 = RMB 8,9640.

Despite ethical considerations, a person's life is measured for rational decision-making. The monetized life loss (M_L) is calculated as the product of the probability of life loss and the value of human life (V_L), while V_L is calculated as the product of GDP_p and the average longevity (L) (Jonkman, 2007). For instance, GDP_p and L in Mianyang City in 2008 are RMB 13,745 and 75 years (Mianyang Bureau of Statistics, 2009). Thus, V_L was RMB 1.03 million.

WARNING DECISION-MAKING FOR THE 2008 TANGJIASHAN LANDSLIDE DAM

Background of the Tangjiashan Landslide Dam

The Tangjiashan landslide lies on the right bank of the Tongkou River in Sichuan Province, China, 4.5 km upstream of Beichuan County (104° 25′56.93″ E, 31°50′40.60″ N) (Xu et al., 2013). The Tongkou River is a tributary of the Fujiang River with a length of 173 km and a basin area of 4,520 km^2. The strata of the Tangjiashan landslide area comprises the upper Qingping Formation of the lower Cambrian dipping outward (N60°E/NW∠60°), a residual-diluvial layer of Quaternary sediments, and an alluvial layer of Quaternary sediments with a depth of 5–20 m in thickness (Xu et al., 2013). The landslide was triggered by the 2008 Ms 7.9 Wenchuan earthquake. The top elevation of the Tangjiashan landslide was 1,580 m, with a slope height of about 900 m. The lower terrain was steep (40°–60°) with the bedrock exposed, whereas the upper terrain gently slopes at an angle of about 30°, with diluvial gravel soil (about 5–15 m in thickness) covering the surface. Details of the landslide refer to (Hu et al., 2009; Xu et al., 2013).

The Tangjiashan landslide slid into the Tongkou River and formed a landslide dam with a height of 82 m, width of 802 m, length of 611 m, dam volume of 20.4 million m^3, and lake capacity of 316 million m^3 (Hu et al., 2009; Cui et al., 2009), as shown in **Table 5**. The landslide dam was located at 4.5 km upstream of Beichuan Town with 30,000 residents and around 85 km upstream of Mianyang City with 1,127,000 residents (**Figure 5A**). The dam mainly consists of three layers (**Figures 5B,C**): the upper layer of gravely soils with a thickness of 5–15 m, the middle layer of strongly weathered cataclasite with a thickness of 10–15 m, and the bottom layer of weakly weathered cataclasite with a thickness of 50–80 m (Peng and Zhang, 2012c; Peng and Zhang, 2013b). The cross-sections of A-A and B-B in **Figure 5** refer to **Figure 6**.

TABLE 5 | Breaching parameters of the two simulation scenarios using DABA and the records.

Breaching parameters	Simulation scenarios		Records
	Scenario 1	Scenario 2	
Breach depth (m)	43.4	42.2	42
Breach top width (m)	204.4	242.5	145–235
Breach bottom width (m)	131.6	171.6	80–100
Breaching time (hour)	14.6	9.6	14
Peak outflow rate (m^3/s)	6,603	14,658	6,500

The risk of dam breaching was high, so the local government decided to excavate a division channel. The division channel was completed by June 1, 2008, with a length of 475 m, a width of 25 m and a depth of 12 m (Peng and Zhang, 2012c; Peng and Zhang, 2013b). It lowered the crest elevation from 752.2 to 740.4 m and reduced the lake capacity from 316 million m^3 to 247 million m^3 (Peng and Zhang 2013b).

The dam breached on June, 10, 2008 and lasted for 14 h. Its peak outflow rate reached 6,500 m^3/ s. The final breach size had a depth of 42 m, a top width of 145–235 m, and a bottom width of 80–100 m (Peng and Zhang, 2012b; Peng and Zhang, 2012c). All the people (30,000) in Beichuan County and 300,000 people in Mianyang City were evacuated by June, 1, 2008, 10 days before the dam breaching. The evacuation costs were estimated as much as RMB 1.2 billion.

Simulation of Dam Breaching and Flood Routing

In order to find out the effect of the channel, two scenarios are simulated, with the division channel (real case of Scenario 1) and without it (a virtual case of Scenario 2). The dam heights of the two scenarios are 70 and 82 m, and the corresponding lake volumes are 224 and 316 million m^3.

A breaching model for landslide dams, DABA (Chang and Zhang, 2010; Peng et al., 2014; Shi et al., 2015), was applied to simulate the dam breaching process and achieve the breaching outflow rate. DABA simulates the soil erosion during dam breaching based on shallow water flow theory. The outflow rate is calculated using the broad-crested weir equations. DABA also takes into consideration the variation of soil properties along with landslide dam depth. The model was proved to be an effective tool for breaching simulation of landslide dams (Chang and Zhang, 2010; Peng et al., 2014; Shi et al., 2015).

HEC-RAS 4.1, a hydraulic simulation software (HEC, 2008), is used to simulate the flood routing after obtaining the breaching outflow rate *via* DABA. Two residential areas downstream are considered in this study: Beichuan County with 30 thousand residents located 4.5 km downstream and Mianyang City with more than 1.1 million residents located 85 km downstream. The main parameters include the dam breaching parameters (the final breach size, breaching time, and breaching progression curve obtained from DABA model), the geometric parameters of the channel, Manning's n values, and contraction and expansion

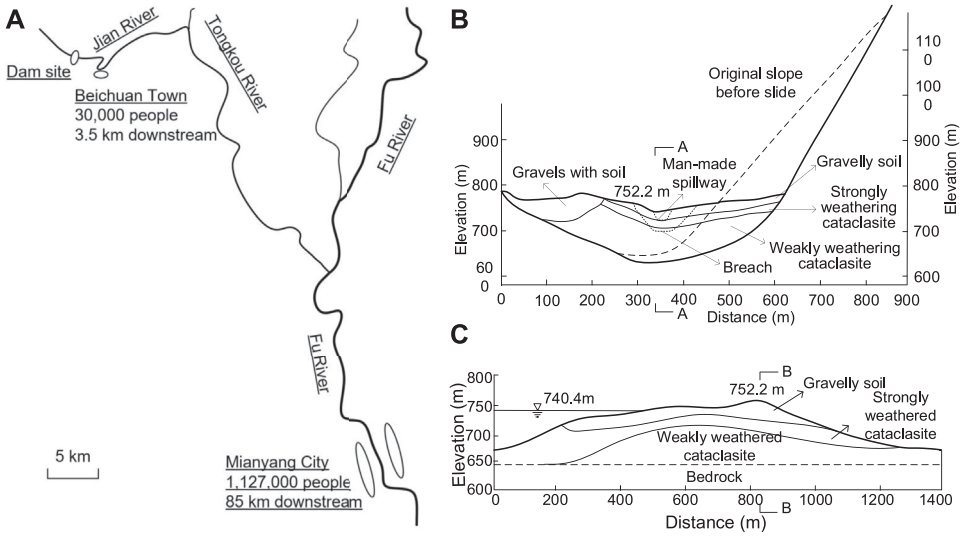

FIGURE 5 | The location and cross-section of the Tangjiashan landslide dam: **(A)** the location of the dam and the Beichuan Town; **(B)** the cross-section across the river; and **(C)** the cross-section along the river (Modified from Peng and Zhang, 2012b and Shi et al., 2015). Note that the cross-sections of A-A and B-B refer to **Figure 6**.

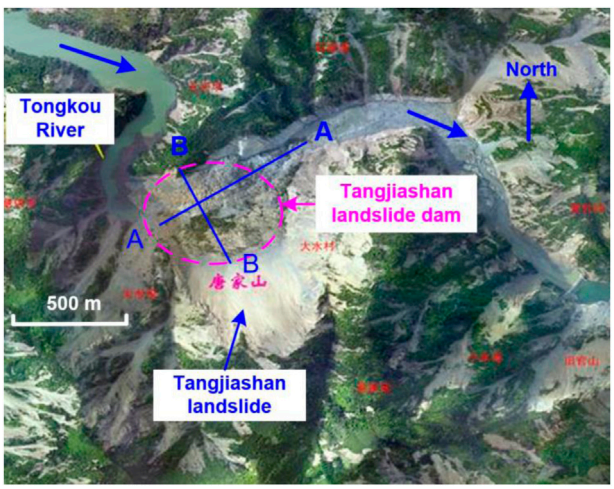

FIGURE 6 | The aerial photograph of the Tangjiashan landslide dam (Modified from Shi et al., 2015).

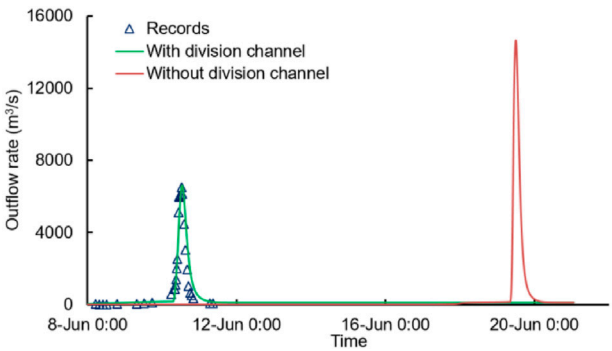

FIGURE 7 | The breaching outflow rates of the real case and two simulated cases.

coefficients. Manning's n values are 0.040 and 0.050 for the channel and the floodplain upstream of Mianyang City, respectively, and 0.035 and 0.045 for the channel and the floodplain in the Mianyang City, respectively, according to Chow (1959).

Figure 7 shows the simulated outflow rates of the two scenarios and the recorded values. With the division channel, the outflow rate curve of the simulated case with the division channel is close to the real case. The peak outflow rate is 6,603 m^3/s and the breach depth is 43.4 m, which are quite close to the records of 6,500 m^3/s and 42 m, respectively (as shown in **Table 5**). Without the division channel, the dam would breach 9 days later due to the larger lake capacity for water filling. The peak outflow rate reaches 14,658 m^3/s, which is much larger than that in Scenario 1. Besides, the final breach size would be slightly shallower but much wider.

The hydraulic parameters in Beichuan County and Mianyang City were obtained *via* HEC-RAS software. In Scenario 1, the flood with the peak flow rate of 6,538 m^3/s inundated Beichuan County with a maximum water depth of 6.13 m (**Figure 8A**) and flow velocity of 1.11 m/s. In Mianyang City, however, the peak flow rate (7,820 m^3/s) was lower than the design flood (12,000 m^3/s) of the levee system. In Scenario 2, the peak flow rates increased to 14,440 and 14,584 m^3/s in Beichuan County and Mianyang City, respectively. The maximum D_w in Beichuan was as large as 19.68 m (**Figure 8A**), and the flow velocity was 1.56 m/s. In Mianyang City, the flood would inundate the city with a maximum depth of 0.51 m (**Figure 8B**) and flow velocity of 0.25 m/s.

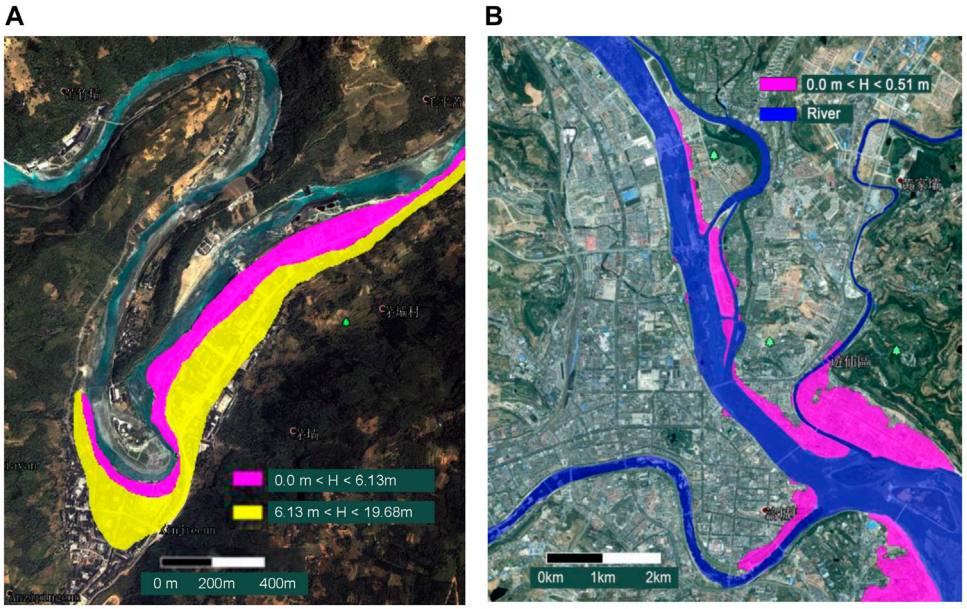

FIGURE 8 | The inundation maps of Beichuan Town and Mianyang City: **(A)** Scenarios 1 (the maximal water level = 6.13 m) and 2 (the maximal water level = 19.68 m) in Beichuan; **(B)** Scenario 2 (the maximal water level = 0.51 m) in Mianyang (Mianyang is not flooded in Scenario 1).

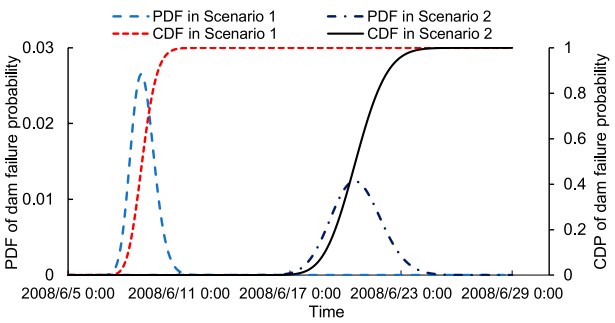

FIGURE 9 | PDF and CDF of P_f in the two Scenarios.

Probability Analysis of Tangjiashan Landslide Dam Failure

As 92% of past landslide dam failures were due to overtopping (Peng and Zhang, 2012c), only overtopping failure is considered in this study. A dam is defined as an overtopping failure at time t when the reservoir volume (V_t) is larger than its capacity (V_{cr}). P_f as a time series is expressed as follows (Peng and Zhang, 2013a):

$$P_f(t) = P[V(t) > V_{cr}]. \tag{24}$$

According to the conservation of mass, $V(t)$ is given by

$$V(t) = V(t - \Delta t) + [Q(t) - Q_o(t) - Q_e(t)]\Delta t, \tag{25}$$

where Δt is the time interval; $Q(t)$ is the inflow rate at time t; $Q_e(t)$ is the evaporation rate, which could be ignored for a short time during the emergency management; $Q_o(t)$ is the outflow rate at time t, which was less than 1 m^3/ s and ignored in this study (Peng and Zhang, 2013b). Thus, $Q(t)$ is the only key item to calculate $P_f(t)$, according to **Eqs. 19**, **20**.

Based on the 33 recorded data provided by Zhang (2009), a time series model of AR (2) is suitable to estimate $Q(t)$:

$$Q(t) = 0.463Q(t-1) - 0.181Q(t-2) + a(t), \tag{26}$$

where $a(t)$ is the error with the mean value of 0. The variation of $a(t)$ is calculated as follows:

$$\sigma_a^2 = \frac{1}{n-1}\sum_1^n a_t^2. \tag{27}$$

With the estimated $Q(t)$ according to **Eqs. 21**, **22**, P_f of the Tangjiashan landslide dam in Scenarios 1 and 2 were obtained as shown in **Figure 9**. For For more details on the time series analysis method for calculating P_f , refer to Peng and Zhang, 2013a; Peng and Zhang, 2013b.

In Scenario 1, P_f increased from 0 to 1E-5 at 21:00 on June 6, 2008, to 1E-3 at 9:00 on June 6, 2008, to 1E-1 at 6:00 on June 8, 2008, and to 0.964 at 6:00 on June 10, 2008. Note that the dam started to breach at 6:00 on June 10, 2008.

In Scenario 2, the corresponding times for P_f arriving 1E-5, 1E-3, 1E-1, and 0.964 were at 10:00 on June15, at 17:00 on June 16, at 15:00 on June 17, and at 2:00 on June 23, 2008.

Warning Decision-Making for Beichuan County

In Scenario 1, the dam breaching flood with the peak discharge of 6,538 m^3/ s inundated 33.0% of the area of Beichuan County, with the population at risk being 9,905. The D_w and flow velocity were 6.13 and 1.11 m/ s, respectively. The expected total loss (L_T) and

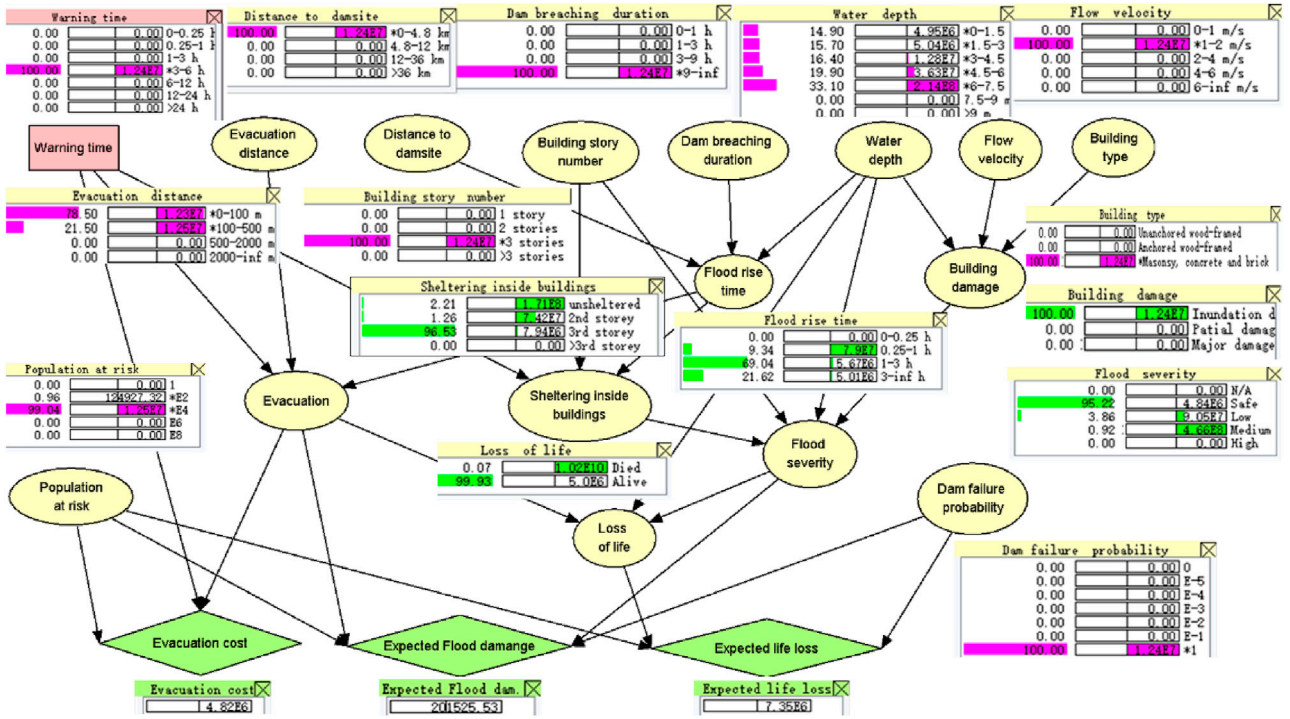

FIGURE 10 | Decision-making based on Influence Diagram with Hugin lite 7.2 (Hugin Expert A/S, 2009).

the three types of flood losses can be obtained by updating the Influence Diagram with the inputs of the basic nodes (without the parent node). **Figure 10** shows an example with the "warning time" of 3–6 h and "dam failure probability" of 1.0. According to the investigation, the six states are deterministic: "flow velocity" (1–2 m/ s), "distance to dam site" (0–4.8 km), "building story number" (3 stories), "dam breaching during" (>9 h), "building type" (masonry, concrete and brick), and "population at risk" (9,905). The states of "water depth" and "evacuation distance" are obtained based on the proportion of the flooded areas (Peng and Zhang, 2013b). In this case, the evacuation rate and the fatality rate are 95.25 and 0.07%, respectively. Since P_{ar} was 9,905, the evacuated population number was 9,435, the exposed population number was 470, and the expected fatality number was 6.9. The evacuation cost, expected flood damage, and expected monetized life loss were 4.82, 2.10, and 7.35 million RMB, respectively, making the expected total loss of 14.3 million RMB, as shown in **Figure 10**.

Table 6 shows the flood losses with P_f = 1.0 in Scenario 1 in Beichuan County with different W_t. When W_t was 0–0.25 h, the evacuation rate was low (35.68%), leading to a relatively high fatality rate (3.71%). The expected monetized life loss of 379 million RMB dominated the total loss, followed by the expected flood damage. With the increase of W_t, both the monetized life loss and the flood damage decreased rapidly and the evacuation cost increased. The expected total loss decreased first and then increased. The minimal expected total loss of 719 million RMB was achieved when the W_t is 6–12 h. After that, the evacuation cost increased steadily and dominated the total loss. The increase in the evacuation cost was due to the larger W_t and more evacuated people.

Figure 11 shows the three types of losses and the total loss in Scenario 1 in Beichuan County with different W_t and P_f. The evacuation cost did not change with P_f. The expected flood damage and monetized life loss linearly decreased with P_f. It is found that the optimal decision strategy with minimal L_T changed with P_f. When P_f = 1, the optimal W_t was 6–12 h with L_T of RMB 7.19 million. With the decrease of W_t, less W_t is needed for optimal decision with less L_T. When P_f = 0.001, no warning is needed since L_T monotonically increases with W_t.

When considering P_f as a time series, as shown in **Figure 9**, the optimal decision is to issue the evacuation warning at 15:00, June 7, 2008, according to **Eq. 11**. It is close to the optimal time of 00: 00, June 7, 2008. The minimal L_T was 3.79 million RMB and P_{fcr} = 0.64%.

In Scenario 2, with the peak discharge of 14,440 m^3/ s, the breaching flood inundated 55.6% of the area of Beichuan County with the population at risk being 16,682. D_w and the flow velocity were 19.68 and 1.56 m/ s, respectively. **Figure 12** shows the three types of losses and the total loss in Scenario 2 in Beichuan County with different W_t and P_f. Similar to Scenario 1, the optimal decision strategy changed with P_f in the trend, which meant less W_t is needed for smaller P_f. However, more W_t and larger L_T are needed in Scenario 2 due to larger floods. When P_f = 1, the optimal W_t was 12–24 h with L_T of RMB 17.90 million. When P_f = 0.001, no warning is needed since L_T monotonically increases with W_t.

When considering P_f as a time series, as shown in **Figure 9**, the optimal decision was to issue the evacuation warning at 6:00, June

TABLE 6 | Flood losses in Scenario 1 in Beichuan County with different W_t.

Warning time	Evacuation rate (%)	Fatality rate	Flood loss (million RMB)			
			Evacuation cost	Expected flood damage	Expected monetized life loss	Expected total loss
0–0.25 h	35.68	3.71%	1.19E+00	1.20E+01	3.79E+02	3.92E+02
0.25–1 h	46.54	3.07%	1.64E+00	8.83E+00	3.13E+02	3.23E+02
1–3 h	74.10	1.16%	3.02E+00	2.67E+00	1.18E+02	1.24E+02
3–6 h	95.26	0.07%	4.82E+00	2.02E-01	7.35E+00	1.24E+01
6–12 h	99.54	2.63E-5	6.82E+00	1.03E-01	2.68E-01	**7.19E+00**
12–24 h	99.98	8.45E-7	1.04E+01	3.48E-04	8.62E-03	1.04E+01
>24 h	100.00	0	1.76E+02	0	0	1.76E+02

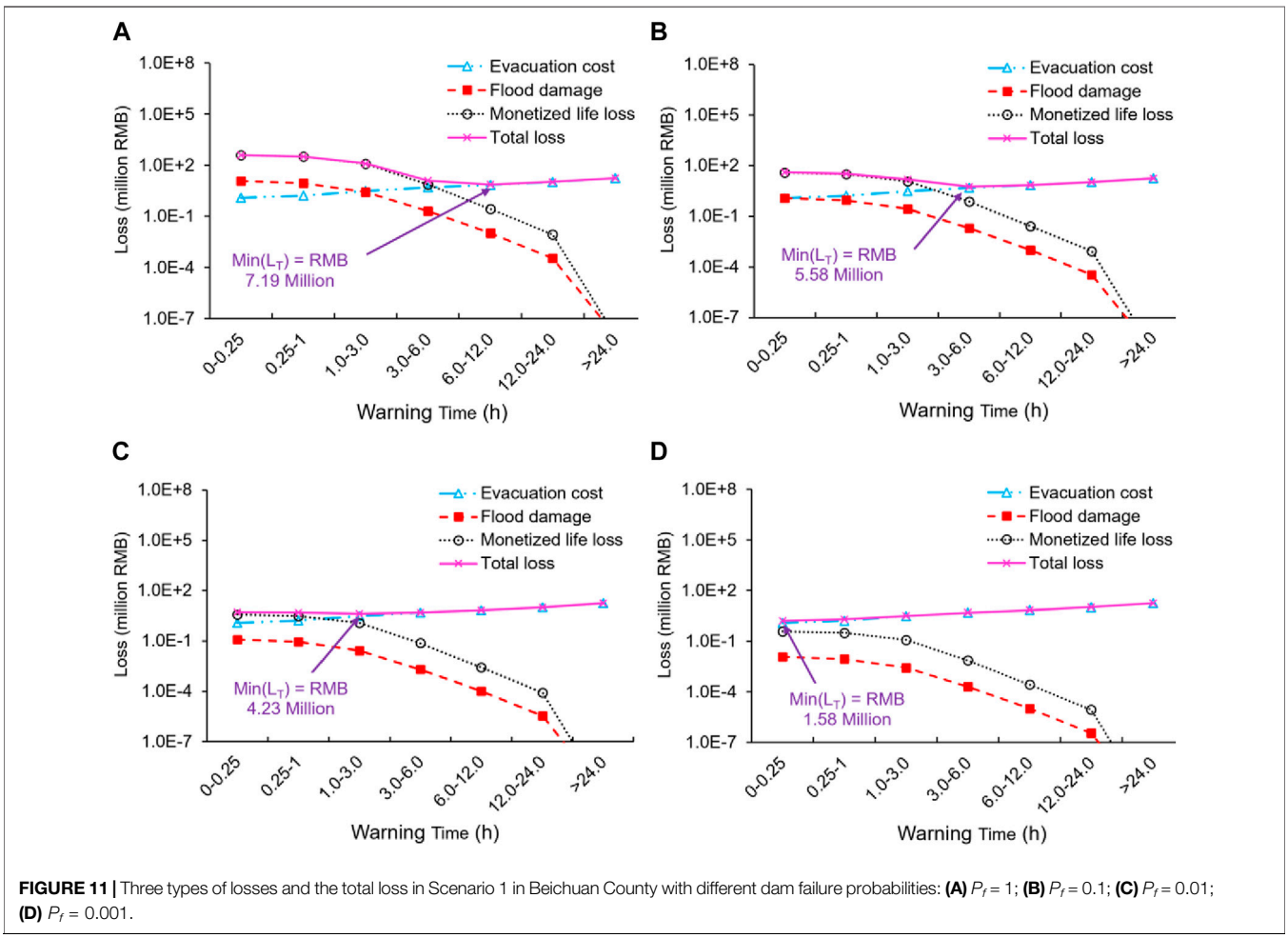

FIGURE 11 | Three types of losses and the total loss in Scenario 1 in Beichuan County with different dam failure probabilities: **(A)** $P_f = 1$; **(B)** $P_f = 0.1$; **(C)** $P_f = 0.01$; **(D)** $P_f = 0.001$.

17, 2008, according to **Eq. 12**. It is close to the optimal time of 08: 00, June 16, 2008. The minimal L_T was 8.95 million RMB and P_{fcr} = 0.49%.

Warning Decision-Making for Mianyang City

In Mianyang City, the breaching flood in Scenario 1 did not inundate the city since the peak discharge (7,820 m^3/ s) was lower than the design value of the levee system (12,000 m^3/ s). The breaching flood in Scenario 2, with the peak discharge of 14,584 m^3/ s, inundated the city with the maximal D_w of 0.51 m and made 23,521 people at risk.

Figure 13 shows the flood loss with different W_t and P_f in Scenario two in Mianyang City. When $P_f = 1$, early warning was necessary despite relatively low flood severity. If W_t is the least, namely 0–0.25 h, L_T would be RMB 13.8 million, which consisted of evacuation cost (C), expected flood damage (D_M) and monetized life loss (M_L) of RMB 5.69, 5.62, and 2.45 million, respectively. With the increase of W_t, D_M and M_L decraese

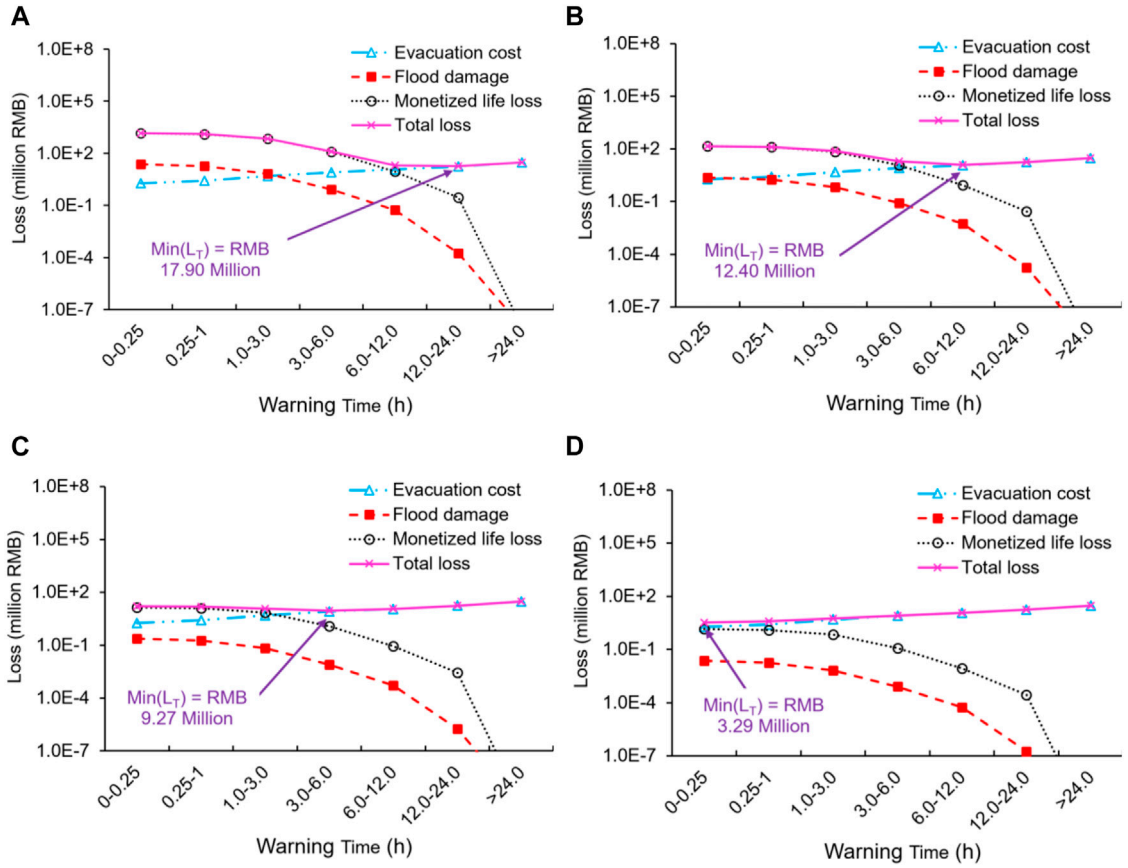

FIGURE 12 | The three types of losses and the total loss in Scenario 2 in Beichuan County with different W_t: **(A)** $P_f = 1$; **(B)** $P_f = 0.1$; **(C)** $P_f = 0.01$; **(D)** $P_f = 0.001$.

dramatically, but C increases rapidly, making L_T decreases first and then increases at W_t = 1–3 h. The minimal L_T at that time is RMB 9.82 million. When P_f became smaller, no warning is needed. The minimal L_T is achieved with W_t = 0–0.25 h as RMB 6.50, 5.77 and 5.70 million in the cases of P_f = 0.1, 0.01 and 0.001, respectively.

When considering the P_f as a time series as shown in **Figure 9**, the optimal decision is to issue the evacuation warning at 22:00, June 19, 2008 according to **Eq. 12**. It is close to optimal time of 10: 00, June 19, 2008. The minimal L_T was 8.17 million RMB and P_{fcr} = 0.307.

DISCUSSION

The Influences of Warning Time, Water Depth, and Dam Failure Probability

The Influence Diagram model (**Figures 4**, **10**) shows that W_t, D_w, and P_f are three key parameters affecting all three types of flood consequences. Sensitivity analysis of W_t, D_w, and P_f on the expected total loss is made in Scenario 1 in Beichuan County.

When P_f = 1, as shown in **Figure 14A**, the expected total loss increased significantly with D_w when W_t was insufficient (e.g., 0–3 h). The reason is that high D_w incurs higher flood severity, building inundation, and damage, which then result in more life loss and flood damage. When W_t becomes longer (e.g., >12 h), the expected total loss, which was dominated by the evacuation costs, would not be obviously influenced by D_w, since most people manage to evacuate from the flooded area.

When P_f decreased, the expected total loss decreased significantly when W_t was insufficient, especially with higher D_w. The optimal decision strategy changed with P_f. Less W_t was needed with smaller P_f. When P_f = 0.001, the expected total loss curve was close to the evacuation cost curve. The reason was that two types of flood losses (expected flood damage and life loss) were proportional to P_f , while evacuation cost did not change with P_f.

In summary, the influences of the three factors (D_w, W_t, and P_f) on the flood losses were different. The increase of D_w resulted in a high increase in the expected flood damage and life loss and a slight decrease in evacuation cost (due to a lower evacuation rate). The increase of P_f resulted in a proportional increase of expected flood damage and life loss but did not change evacuation costs. The increase of W_t resulted in a steady increase in evacuation cost but incurred an unsteady decrease of expected flood damage and life loss. The latter decreased rapidly when W_t was not sufficient. In contrast, they change a little when W_t was sufficient.

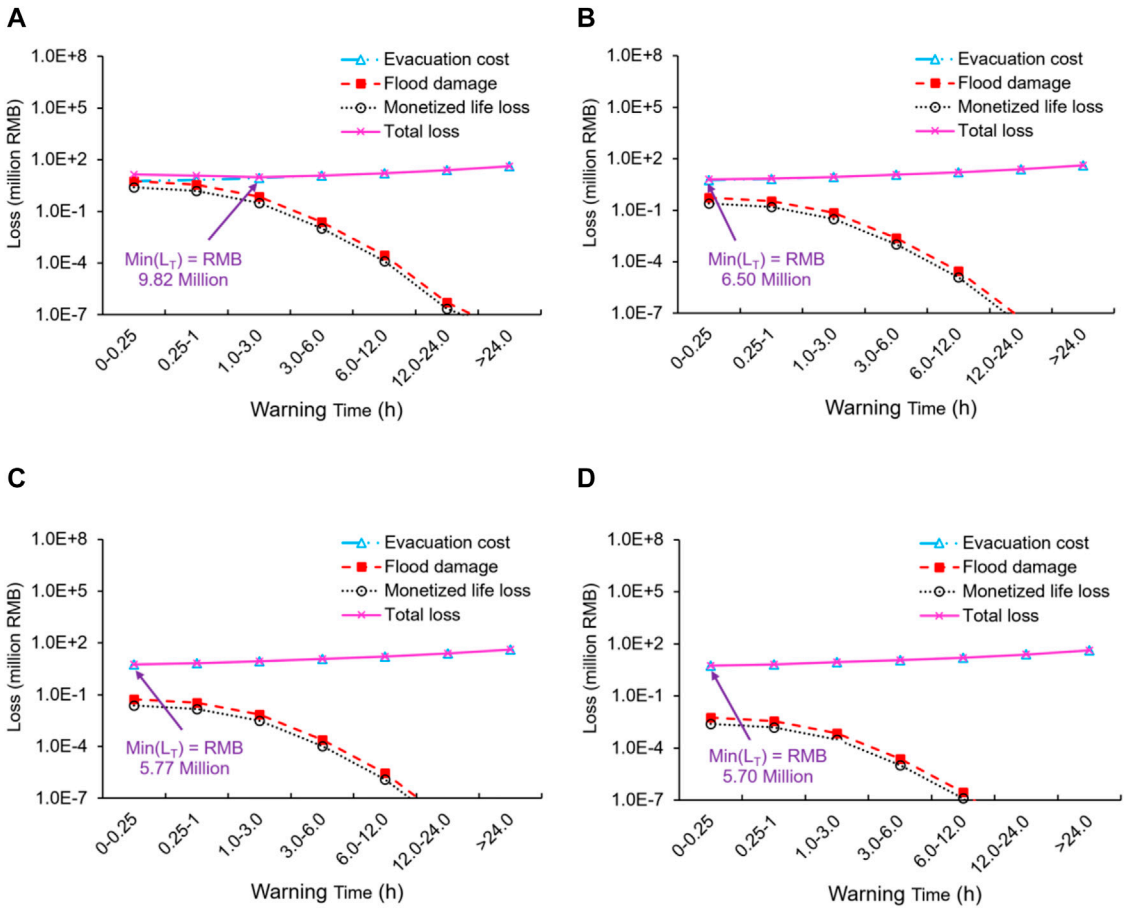

FIGURE 13 | The three types of losses and the total loss in Scenario 2 in Mianyang City with different W_t: **(A)** P_f = 1; **(B)** P_f = 0.1; **(C)** P_f = 0.01; **(D)** P_f = 0.001.

Comparison DEMID With Decision Tree

Frieser (2004) has published decision-making methods for dam/levee failure flood *via* multi-phase decision tree, as shown in **Figure 15**. At the initiation decision time t_i, we might issue an evacuation warning or not. If we choose not, we might delay the decision to t_τ. Since there are several phases that we can choose to make the warning decision, it is called a multi-phase decision tree, as shown in **Figure 15**. It involves P_f and three types of flood losses. A warning decision was made by comparing all the alternatives to achieve the minimum expected total loss.

Compared to the multi-phase decision tree method, DEMID has several features:

1) The inter-relationships of influence factors are qualitatively analyzed using Influence Diagram. The inter-relationships of influence factors are qualitatively analyzed by building an Influence Diagram with causality connections and quantitatively analyzed with conditional probabilities. Moreover, all alternatives in decision trees are assumed as independent and the inter-relationships of influence factors are neglected.
2) Multi-source information is absorbed to improve DEMID. Prior (conditional) probabilities are gained by employing multi-source information, such as physical test data, empirical equations, theoretical analysis, and statistical data. The information of the studied case can be applied to calculate the posterior probabilities. Moreover, the model can be further updated through Bayesian network parameter learning in the future.
3) The probabilities of the influence factors, including the basic nodes and intermediate nodes, can be obtained through inversion analysis based on Bayesian theory. Suppose that a failed landslide causes a large number of fatalities and some parameters (e.g., W_t and the building information) are gained, we can find the distribution of D_w and evacuation based on Bayesian updating by simply inputting the fatality rate and other known parameters.
4) From the perspective of the building process, DEMID is built according to the logical relationship between the influence factors (nodes), which cannot be reflected in the decision tree. The latter simply divides the alternatives as binary variables, namely, warning or non-warning. In the application prospect,

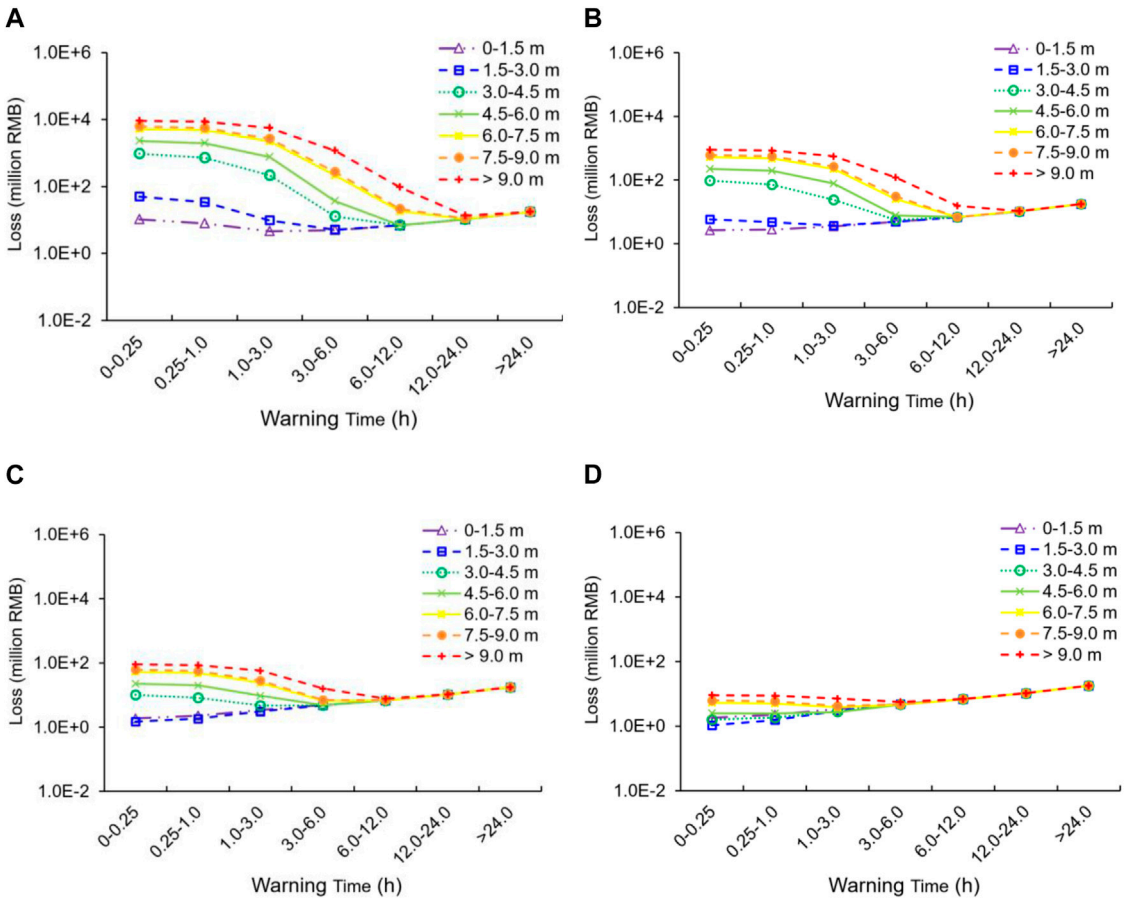

FIGURE 14 | The expected total loss in Scenario 1 in Beichuan County with different D_w and W_t: **(A)** P_f = 1; **(B)** P_f = 0.1; **(C)** P_f = 0.01; **(D)** P_f = 0.001.

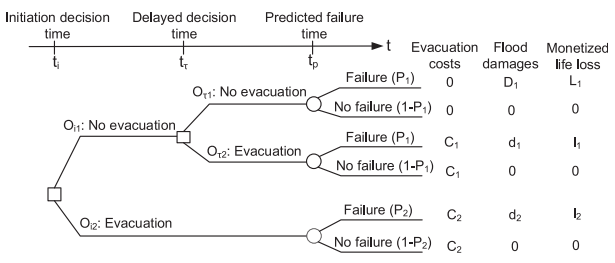

FIGURE 15 | Multi-phase decision trees for warning decision-making of dam/levee failure. Note $D_1 > d_1 > d_2$, $L_1 > l_1 > l_2$, $C_2 > C_1$ for different W_t and the uncertainty of P_1 is smaller than that of P_2 since more information can be gained.

the decision tree needs to assume a fixed failure time, while it is not necessary for DEMID.

Comparing DEMID With a Dynamic Decision-Making Model, DYDEM

Peng and Zhang (2013a) and Peng and Zhang (2013b) have provided a dynamic decision-making model (DYDEM) for dam failure warnings. The warning decision strategy was to find the time of evacuation warning to minimize expected total loss:

$$Min[E(L_T(t_w))] \Leftrightarrow \frac{dE[L_T(t_w)]}{dt_w} = 0, \tag{28}$$

where t_w is the time issuing warning and $L_T(t_w)$ is the expected total loss as a function of t_w, which can be expressed as follows:

$$\begin{aligned} E[L_t(t_w)] &= \int L_t(t_w) f(t_f) dt_f \\ &= \int_{t_0}^{+\infty} C(W_t) f(t_f) dt_f + \int_{t_0}^{+\infty} [D_M(W_t) \\ &\quad + M_L(W_t)] f(t_f) dt_f, \end{aligned} \tag{29}$$

where t_f is the continuous time of failure since a dam could fail at any time with a certain probability; $f(t_f)$ is a continuous stochastic process of P_f, $f(t_f)dt_f$ is P_f in a short period dt. In **Eq. 24**, W_t is expressed as follows:

$$W_t = 0, \text{ when } t_f < t_w; \tag{30}$$

$$W_t = t_f - t_w, \text{ when } t_f \geq t_w. \tag{31}$$

In DEDYM, the expected L_T is calculated with P_f as a time series and the three types of flood losses as a function of W_t. This

model is suitable for detailed case studies with sufficient investigated and simulated parameters. It is time-consuming since P_f and three types of flood losses are calculated *via* different methods. Moreover, the Bayesian network in HURAM with several discrete states cannot be directly applied for calculating the three types of flood losses. A program is coded in VBA in Microsoft Excel for this purpose.

Compared to DYDEM, DEMID has several distinct features:

1) It unifies all the component methods in DYDEM *via* Influence Diagram. In DYDEM, P_f is calculated *via* a time series method, the evacuation rate and fatality rate are calculated *via* HURAM; the evacuation cost, flood damage, and monetized life loss are calculated *via* different methods. DYDEM is suitable for detailed case studies with sufficient investigated and simulated parameters. However, it may not be sufficient for some short-lived landslide dam cases. In DEMID, all the components are unified using only one method, Influence Diagram. The three types of flood loss and the expected total loss can be directly gained.
2) DEMID is more efficient. Besides the unified form discussed above, the integration calculation as shown in **Eq. 24** in DYDEM is not needed in DEMID and the decision criteria are much simpler. We only need to check the critical failure probability P_{fcr}, as shown in **Eq. 12**, to find the optimal time for issuing a warning. An important premise for the correctness of the criterion is that P_f should monotonically increase with time. This is not difficult to achieve in landslide dam cases since no discharge control measures are available for a naturally formed dam.
3) DEMID can conduct inversion analysis based on Bayesian theory, as discussed in the last section. Since Influence Diagram is an updated Bayesian network, DEMID retains the original advantages of the Bayesian network in HURAM. We can find out the causes (e.g., water depth and breaching time) of one or some results (e.g., high fatality rate and evacuation rate). This cannot be realized in DYDEM.
4) From the perspective of the building process, the structures of DEMID and all the nodes are fixed. The model can be applied to any landslide dam case by simply updating the values of the basic nodes (the nodes without parents). In DYDEM, we need to calculate all the risk components (dam failure probability and the three types of losses) in all sub-areas by different methods. Then sum all the losses in all sub-areas to gain the expected total loss.

CONCLUSIONS

A new warning decision-making model (DEMID) is presented based on Influence Diagram in this article. It is used for the emergent warning decision-making in the case of the 2008 Tangjiashan landslide dam. The following conclusions can be drawn:

1) The present decision model is of great efficiency as it unifies the dam failure probability, evacuation, and three types of flood losses in one Influence Diagram. The expected total loss can be directly gained. Besides, a warning criterion is suggested for efficient decision-making by considering the monotonical increase of landslide dam failure probability: issuing the warning at the time with critical probability when no warning is no more the best choice (with minimal expected total loss).
2) In DEMID, the inter-relationships of influence factors are qualitatively analyzed with causality connections and quantitatively analyzed with conditional probabilities. Continuous values of the population at risk and failure probability can be considered by weighted averages of the closest discrete states. The probabilities of the influence factors, including the basic nodes and intermediate nodes, can be obtained through inversion analysis based on Bayesian theory.
3) The increase of water depth results in a high increase in the expected flood damage and life loss and a slight decrease in evacuation cost (due to a lower evacuation rate). The increase of P_f results in a proportional increase in expected flood damage and life loss but no changes to evacuation cost. The increase of W_t results in a steady increase in evacuation cost and an unsteady decrease in expected flood damage and life loss. The latter decreases rapidly when W_t is not sufficient but changes slightly when W_t is sufficient.
4) For the high-risk areas with relatively fewer people (e.g., the Beichuan County), the expected total loss is dominated by monetized life loss. It is better to issue an evacuation warning a little earlier since it would not incur large evacuation expenses but save many human lives. For the low-risk areas with relatively more people (e.g., the Mianyang City), the evacuation cost should be cautiously issued since the longer the warning lasts, the larger the expenses are.

DATA AVAILABILITY STATEMENT

The original contributions presented in the study are included in the article/supplementary material; further inquiries can be directed to the corresponding authors.

AUTHOR CONTRIBUTIONS

YZ wrote the original draft and performed the calculation and analysis. MP contributed to the conceptualization, supervision, methodology, and funding acquisition. PZ was responsible for the writing of the original draft and funding acquisition. LZ contributed to the conceptualization and obtaining the resources and reviewed and edited the manuscript.

FUNDING

The authors acknowledge the support from the Shanghai Rising-Star Program (20QB1406000), the National Natural Science Foundation of China (41877234, 41731283, 42071010, 4201101075), the Natural Science Foundation of Shandong province (Grant No. ZR2019QEE008), and the Fundamental Research Funds for the Central Universities.

REFERENCES

Acosta-Coll, M., Ballester-Merelo, F., Martinez-Peiró, M., and De la Hoz-Franco, E. (2018). Real-time Early Warning System Design for Pluvial Flash Floods-A Review. *Sensors* 18 (7), 2255. doi:10.3390/s18072255

ANCOLD (1998). *Guidelines on Risk Assessment. Working Group on Risk Assessment*. Sydney, New South Wales, Australia: Australian National Committee on Large Dams.

Chang, D. S., and Zhang, L. M. (2010). Simulation of the Erosion Process of Landslide Dams Due to Overtopping Considering Variations in Soil Erodibility along Depth. *Nat. Hazards Earth Syst. Sci.* 10 (4), 933–946. doi:10.5194/nhess-10-933-2010

Chow, V. T. (1959). *Open Channel Hydraulics*. New York: McGraw-Hill Book Company.

Correa, O., García, F., Bernal, G., Cardona, O. D., and Rodriguez, C. (2020). Early Warning System for Rainfall-Triggered Landslides Based on Real-Time Probabilistic hazard Assessment. *Nat. Hazards* 100 (1), 345–361. doi:10.1007/s11069-019-03815-w

Cui, P., Zhu, Y.-y., Han, Y.-s., Chen, X.-q., and Zhuang, J.-q. (2009). The 12 May Wenchuan Earthquake-Induced Landslide Lakes: Distribution and Preliminary Risk Evaluation. *Landslides* 6 (3), 209–223. doi:10.1007/s10346-009-0160-9

Fan, Q., Tian, Z., and Wang, W. (2018). Study on Risk Assessment and Early Warning of Flood-Affected Areas when a Dam Break Occurs in a Mountain River. *Water* 10 (10), 1369. doi:10.3390/w10101369

Fan, X., Xu, Q., Alonso-Rodriguez, A., Subramanian, S. S., Li, W., Zheng, G., et al. (2019). Successive Landsliding and Damming of the Jinsha River in Eastern Tibet, China: Prime Investigation, Early Warning, and Emergency Response. *Landslides* 16, 1003–1020. doi:10.1007/s10346-019-01159-x

FEMA (2004). *Federal Guidelines for Dam Safety – Hazard Potential Classification System for Dams*. Washington, USA: Federal Emergency Management Agency. Federal Emergency Management Agency.

Frieser, B. (2004). *Probabilistic Evacuation Decision Model for River Floods in the Netherlands*. Delft, Netherlands: Delft University of Technology, 138p. Final report.

Grant, S., and Nover, J. (2019). Diagnosis of Historical Inundation Events in the Marshall Islands to Assist Early Warning Systems. *Nat. Hazards* 99 (1), þ189–216. doi:10.1007/s11069-019-03735-9

HEC (2008). HEC-RAS, River Analysis System, Hydraulic Reference Manual, Version 4.0, *Developed by Hydrologic Engineering*. Washington DC, USA: Center of US Army Corps of Engineers. Hydrologic Engineering Center.

Howard, R. A., and Matheson, J. E. (2005). Influence Diagrams. *Decis. Anal.*, 2(3): 127–143. doi:10.1287/deca.1050.0020

Hu, X. W., Huang, R. Q., Shi, Y. B., Lu, X. P., Zhu, H. Y., and Wang, X. R. (2009). Analysis of Blocking River Mechanism of the Tangjiashan Landslide and Dam-Breaking Mode of its Barrier Dam. *Chin. J. Rock Mech. Eng.* 28 (1), 181–189. in Chinese. doi:10.1002/9780470611807.ch2

Hugin Expert A/S. (2009). Hugin Lite. Available at: http://www.hugin.com/Products_Services/Products/Demo/Lite/ (Accessed Jan 20, 2009).

Hydro, B. C. (1993). *Guidelines For Consequence-Based Dam Safety Evaluations And Improvements*. Canada: Hydroelectric Engineering Division Report No. H2528, BC Hydro, Burnaby, BC.

Jensen, F. V. (2001). *Bayesian Networks and Decision Graphs*. New York: Springer. doi:10.1007/978-1-4757-3502-4

Jonkman, S. N. (2007). *Loss of Life Estimation in Flood Risk Assessment: Theory and Applications*. Delft, Netherlands: Ph. D. Thesis, Delft University of Technology. doi:10.1142/9789812709554_0118

Li, M.-H., Sung, R.-T., Dong, J.-J., Lee, C.-T., and Chen, C.-C. (2011). The Formation and Breaching of a Short-Lived Landslide Dam at Hsiaolin Village, Taiwan - Part II: Simulation of Debris Flow with Landslide Dam Breach. *Eng. Geology.* 123 (1–2), 60–71. doi:10.1016/j.enggeo.2011.05.002

Li, W., Ye, Y. C., Hu, N. Y., Wang, X. H., and Wang, Q. H. (2019). Real-Time Warning and Risk Assessment of Tailings Dam Disaster Status Based on Dynamic Hierarchy-Grey Relation Analysis. *Complexity* 2019, 1–14. 5873420. doi:10.1155/2019/5873420

Lindell, M. K., Prater, C. S., and Peacock, W. G. (2007). Organizational Communication and Decision Making for hurricane Emergencies. *Nat. Hazards Rev.* 8 (3), 50–60. doi:10.1061/(asce)1527-6988(2007)8:3(50)

Liu, C. J., Guo, L., Ye, L., Zhang, S. F., Zhao, Y. Z., and Song, T. Y. (2018). A Review of Advances in China's Flash Flood Early-Warning System. *Nat. Hazards* 92 (2), 619–634. doi:10.1007/s11069-018-3173-7

Liu, N., Chen, Z., Zhang, J., Lin, W., Chen, W., and Xu, W. (2010). Draining the Tangjiashan Barrier lake. *J. Hydraul. Eng.* 136 (11), 914–923. doi:10.1061/(asce)hy.1943-7900.0000241

Mandal, A. K., Ramakrishnan, R., Pandey, S., Rao, A. D., and Kumar, P. (2020). An Early Warning System for Inundation Forecast Due to a Tropical Cyclone along the East Coast of India. *Nat. Hazards* 103, 2277–2293. doi:10.1007/s11069-020-04082-w

Mianyang Bureau of Statistics (2008). *Report on the National Economy and Society Development on Miangyang City in 2008*. Mianyang Bureau of Statistics, Sichuan Province, China. Available at: http://my.gov.cn/bmwz/94294769050464256/ 20090325/391646.html (Accessed December 20, 2008). (in Chinese).

Nielsen, N. M., Hartford, D. N. D., and MacDonald, J. J. (1994). Selection of Tolerable Risk Criteria for Dam Safety Decision Making. *Proc. 1994 Can. Dam Saf. Conf.* 26 (5), 355–369.

Peng, M., and Zhang, L. M. (2012c). Analysis of Human Risks Due to Dam Break Floods - Part 1: A New Model Based on Bayesian Networks. *Nat. Hazards* 64 (1), 903–933. doi:10.1007/s11069-012-0275-5

Peng, M., and Zhang, L. M. (2012b). Analysis of Human Risks Due to Dam Break Floods-Part 2: Application to Tangjiashan Landslide Dam Failure. *Nat. Hazards* 64 (2), 1899–1923. doi:10.1007/s11069-012-0336-9

Peng, M., and Zhang, L. M. (2012a). Breaching Parameters of Landslide Dams. *Landslides* 9 (1), 13–31. doi:10.1007/s10346-011-0271-y

Peng, M., Zhang, L. M., Chang, D. S., and Shi, Z. M. (2014). Engineering Risk Mitigation Measures for the Landslide Dams Induced by the 2008 Wenchuan Earthquake. *Eng. Geology.* 180, 68–84. doi:10.1016/j.enggeo.2014.03.016

Peng, M., and Zhang, L. M. (2013a). Dynamic Decision Making for Dam-Break Emergency Management - Part 1: Theoretical Framework. *Nat. Hazards Earth Syst. Sci.* 13 (2), 425–437. doi:10.5194/nhess-13-425-2013

Peng, M., and Zhang, L. M. (2013b). Dynamic Decision Making for Dam-Break Emergency Management - Part 2: Application to Tangjiashan Landslide Dam Failure. *Nat. Hazards Earth Syst. Sci.* 13 (2), 439–454. doi:10.5194/nhess-13-439-2013

Shen, D. Y., Shi, Z. M., Peng, M., Zhang, L. M., and Jiang, M. Z. (2020). Longevity Analysis of Landslide Dams. *Landslides* 17 (8), 797–1821. doi:10.1007/s10346-020-01386-7

Shi, Z. M., Guan, S. G., Peng, M., Zhang, L. M., Zhu, Y., and Cai, Q. P. (2015). Cascading Breaching of the Tangjiashan Landslide Dam and Two Smaller Downstream Landslide Dams. *Eng. Geology.* 193, 445–458. doi:10.1016/j.enggeo.2015.05.021

Shi, Z. M., Xiong, X., Peng, M., Zhang, L. M., Xiong, Y. F., Chen, H. X., et al. (2017). Risk Assessment and Mitigation for the Hongshiyan Landslide Dam Triggered by the 2014 Ludian Earthquake in Yunnan, China. *Landslides* 14 (1), 1–17. doi:10.1007/s10346-016-0699-1

Smith, P. J., Kojiri, T., and Sekii, K. (2006). *Risk-based Flood Evacuation Decision Using a Distributed Rainfall-Runoff Model*. Kyoto, Japan: Annuals of Disas. No. 49 B.

Su, H., Wen, Z., and Wu, Z. (2011). Study on an Intelligent Inference Engine in Early-Warning System of Dam Health. *Water Resour. Manage.* 25, 1545–1563. doi:10.1007/s11269-010-9760-3

Su, H., Wen, Z., Yan, X., Liu, H., and Yang, M. (2018). Early-warning Model of Deformation Safety for Roller Compacted concrete Arch Dam Considering Time-Varying Characteristics. *Compos. Structures* 203, 373–381. doi:10.1016/j.compstruct.2018.07.023

Urbina, E., and Wolshon, B. (2003). National Review of hurricane Evacuation Plans and Policies: a Comparison and Contrast of State Practices. *Transportation Res. A: Pol. Pract.* 37 (3), 257–275. doi:10.1016/s0965-8564(02)00015-0

USBR (1997). *Guidelines for Achieving Public Protection in Dam Safety Decision Making*. Denver, CO, USA: Dam Safety Office, US Bureau of Reclamation. US Bureau of Reclamation.

Wang, Y., Li, J., Wu, Z., Chen, J., Yin, C., and Bian, K. (2020). Dynamic Risk Evaluation and Early Warning of Crest Cracking for High Earth-Rockfill Dams through Bayesian Parameter Updating. *Appl. Sci.* 10, 7627. doi:10.3390/app10217627

Woo, G. (2008). Probabilistic Criteria for Volcano Evacuation Decisions. *Nat. Hazards* 45 (1), 87–97. doi:10.1007/s11069-007-9171-9

Xu, W.-J., Xu, Q., and Wang, Y.-J. (2013). The Mechanism of High-Speed Motion and Damming of the Tangjiashan Landslide. *Eng. Geology.* 157, 8–20. doi:10.1016/j.enggeo.2013.01.020

Zhai, X., Guo, L., Liu, R., and Zhang, Y. (2018). Rainfall Threshold Determination for Flash Flood Warning in Mountainous Catchments with Consideration of Antecedent Soil Moisture and Rainfall Pattern. *Nat. Hazards* 94, 605–625. doi:10.1007/s11069-018-3404-y

Zhang, J. X. (2009). *Hydrologic Analysis and Emergency Application of Barrier lake Breaking*. Beijing, China: Ph.D. thesis Tsinghua University. in Chinese. doi:10.1190/1.3603612

Zhang, L. M., Peng, M., Chang, D. S., and Xu, Y. (2016). *Dam Failure Mechanisms and Risk Assessment*. Singapore: Wiley. doi:10.1002/9781118558522

Zhang, L. W., and Guo, H. P. (2006). *Introduction to Bayesian Networks*. Beijing, China: China Science Publishing & Media Ltd. (CSPM). (in Chinese).

Conflict of Interest: Author YZ was employed by the company China Shipbuilding NDRI Engineering Co., Ltd.

The remaining authors declare that the research was conducted in the absence of any commercial or financial relationships that could be construed as a potential conflict of interest.

Publisher's Note: All claims expressed in this article are solely those of the authors and do not necessarily represent those of their affiliated organizations, or those of the publisher, the editors and the reviewers. Any product that may be evaluated in this article, or claim that may be made by its manufacturer, is not guaranteed or endorsed by the publisher.

Copyright © 2021 Zhu, Peng, Zhang and Zhang. This is an open-access article distributed under the terms of the Creative Commons Attribution License (CC BY). The use, distribution or reproduction in other forums is permitted, provided the original author(s) and the copyright owner(s) are credited and that the original publication in this journal is cited, in accordance with accepted academic practice. No use, distribution or reproduction is permitted which does not comply with these terms.